THERMAL AND ELECTRICAL CHARACTERIZATION OF POLYMERIC NANOCOMPOSITES

Bernard Barbosa da Silva
Leandro Alcoforado Sphaier
Universidade Federal Fluminense, Rua Passo da Patria 156, SÃčo Domingos, Niteroi, Rio de Janeiro, Brazil
bbarbosa@id.uff.br; lasphaier@id.uff.br

Michael Hilbert
Technische Universitaet Braunschweig, Schleinitzstrasse 23, Braunschweig, Germany
m.hilbert@tu-bs.de

Abstract. With the advent of nanotechnology, composite systems can present properties way beyond the expected when compared to those composed of bigger scale materials. Therefore, many areas rely on these new features to keep their progress and evolution. The aim of the project is to experimentally characterize nanocomposite systems composed of polymeric resin matrices filled with metal oxide nanoparticles. The material used in the polymeric matrix was the unsaturated polyester resin while the ones used as fillers were two different aluminum oxides. Hence, the electrical permittivity of these composites was experimentally measured using a Schering bridge and the thermal conductivity was measured through a guarded heat flow thermal conductivity meter. Lastly, discussion and theories concerning to the obtained results of the characterization processes and a comparison between the electrical and thermal properties evolution are presented.

Keywords: nanocomposites, electrical permittivity, thermal conductivity, electrical and thermal properties, properties comparison

1. INTRODUCTION

The usage of polymeric materials in the industry, no matter in what area, has considerably grown with the advance of technology and, consequently, with the creation of new means of production and a bigger knowledge of its characteristics. These materials are preferred due to their low weight, good processability at low temperatures, good corrosion resistance and easy handling. The low thermal and electrical conductivities of the polymers are characteristics that make their use indispensable for some applications and at the same time impossible for others. Adding metallic nanoparticles in disperse phase in polymeric matrices can make a significant change in the thermal and electrical characteristics of these matrices. The result obtained from the nanomaterials insertion in polymeric matrices is called nanocomposite. The study of the addition of silver nanoparticles in epoxy resin matrices for thermal conductive adhesive by Fan *et al.* (2004) is an example of the variety of applications that the nanocomposites have in the industry.

Composites of resin matrices filled with metallic oxide particles have been widely researched and used for insulation systems. The electric discharges arising from high voltage equipments can produce chemical, electrical and thermal degradation of the isolating material. Chemical degradation can occour due to the products of ionization, electrical degradation due to the bombardment of ions and electrons, and thermal because of the high temperatures that can be achieved (Alston, 1968). A good insulating material means that it has good dielectric and thermomechanical properties, therefore the composites are the perfect combination for this usage with good thermal properties and high mechanical and breakdown strenghts. With the popularization of nanoparticles, studies of nanocomposites are being done in order to determine if and how better the nanocomposites are when compared to the more commonly used microcomposites for high voltage aplications (Preetha and Thomas, 2011).

The objective of this project is to experimentally characterize nanocomposite systems composed of polymeric resin matrices filled with metal oxide nanoparticles. For this purpose, the electrical permittivity of these composites was experimentally measured using a Schering bridge and the thermal conductivity was measured through a guarded heat flow thermal conductivity meter. Lastly, discussion and theories concerning to the obtained results of the characterization processes and a comparison between the electrical and thermal properties evolution are presented.

2. MATERIALS

2.1 Polymers

Polymers are macromolecules obtained from the repetition of a smaller unit, called monomer. This name, polymer, comes from the Greek and means many parts. These materials are obtained from polymerization reaction and have the following characteristics: high molecular mass, low weight, good processability at low temperatures, good corrosion

resistance and low thermal and electrical conductivities.

2.2 Nanoparticles

A particle is an object that behaves like a whole unit in relation to its transport and properties. Initially called ultrathin particles during studies in the 1970s and 1980s, nanoparticles are those whose diameter is between 1 and 1000 nanometers. The name has been changed during the 1990s as nanoparticles were more fashionable than ultrathin particles.

One characteristic of nanoparticles is that the same material can present different properties if the nanometric and macroscopic scales are compared (ASTM, 2006). These property differences are originated by the nanocrystals and rely on the nanostructure of particles. Nanoparticles are also a big object of study due to their very important interfacial interactions, since many of the atoms of a particle are in its surface because of their small size.

2.3 Nanocomposites

Nanocomposites are materials composed by the union of two or more components where at least one of them has a nanometric scale dimension. The mostly studied nanocomposites are composed by only two materials: a macrometric scale matrix filled with nanometric scale material.

Due to the great interfacial interactions of the nanometric scale dimension components, a homogenous dispersion of these components is capable of generating a composite with characteristics way beyond the observed on the matrix (Rong *et al.*, 2006; Tjong, 2006; Hamming *et al.*, 2009). However, the great interfacial interactions tends to keep the nanoparticles agglomerated reducing the improvements in the characteristics of the matrix. Therefore, a homogenous dispersion of the nanoparticles is vital to maximize the improvements in the characteristics (Kim *et al.*, 2007).

The main advantages offered by nanocomposites are: better electrical, thermal and mechanical properties; higher chemical resistance; reduction in gases permeability; and fireproof property.

Despite of not being used on a large scale by the actual industry, nanocomposites are widely used in the manufacturing of: waterproof textiles, fireproof materials, Thermal Interface Materials (TIM), amongst others.

3. ELECTRICAL PROPERTIES

3.1 Electrical permittivity

The electrical permittivity determines how resistant a dielectric is to form an electric field. The higher the electrical permittivity, the bigger will be the electric field's influence over the dielectric and, consequently, more of this electric field will be transmitted through the dielectric.

The electrical permittivity of a dielectric depends on the vacuum electrical permittivity, ϵ_o, and the relative electrical permittivity of the material ϵ_r.

$$\epsilon = \epsilon_r \epsilon_o \tag{1}$$

The relative electrical permittivity of the polymers at 25°C usually range from 2F/m to 10F/m.

4. THERMAL PROPERTIES

4.1 Thermal conductivity

According to Fourier's Law, the thermal conductivity, k, is a proportionality coefficient that relates the heat flow, $\dot{q}''$, with the temperature gradient, ∇T. The following equation defines Fourier's Law for isotropic materials:

$$\dot{\mathbf{q}}'' = -k\nabla T \tag{2}$$

4.2 Conduction thermal resistance

The thermal resistance follows the same definition as the electrical resistance, but defines how the material opposes to heat flow. It can be used on steady state one-dimensional cases without internal energy generation.

$$R_{cond} = \frac{L}{kA_x} \tag{3}$$

Where R_{cond} is the conduction thermal resistance, L is the length that the heat flow crosses, k is the thermal conductivity and A_x is the section area.

4.2.1 Series arrangement for conduction thermal resistance

Similar to electrical resistances, it is also possible to arrange conduction thermal resistances in series. The total resistance is calculated through the sum of every resistance as defined in equation (3):

$$R_{condt} = R_{cond1} + R_{cond2} + ... + R_{condn} \tag{4}$$

Explicing each thermal resistance:

$$\frac{L_t}{k_t A_{xt}} = \frac{L_1}{k_1 A_{x1}} + \frac{L_2}{k_2 A_{x2}} + ... + \frac{L_n}{k_n A_{xn}} \tag{5}$$

Figure 1 illustrates the analogy between the series arrangement for conduction thermal resistance.
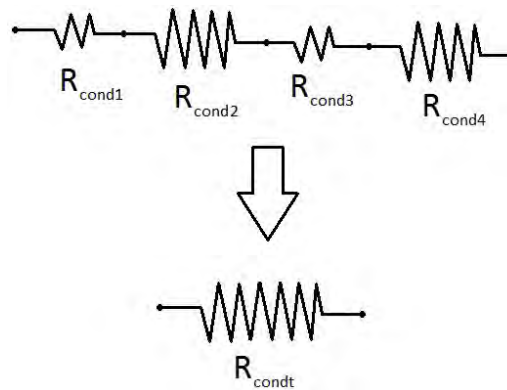

Figure 1. Analogy between the series arrangement for conduction thermal resistance

5. EMPLOYED MATERIALS

5.1 Matrices

The resin used in this work was Reichold's unsaturated polyester resin (UPR) Polylite 10316-10. According to the manufacturer, its density is 1090kg/m^3, its viscosity at 25°C ranges from 250 to 350cP and it has a Heat Distortion Temperature (HDT) of 85°C.

5.2 Fillers

Two different nanoparticles were used as fillers in this work: aluminum oxide with average particle size of 30nm to 40nm (Al_2O_3 30-40), aluminum oxide with average particle size of 200nm (Al_2O_3 200). Table 1 contain their properties according to their manufacturer, Nanostructured And Amorphous Materials, Inc.

Table 1. Nanoparticles properties according to their manufacturer

Material	Density (kg/m^3)	Morphology	Average particle size (nm)	Specific superficial area (10^3 m^2/kg)	Purity
Al_2O_3 30-40	3500 to 3900	Nearly spherical	30 to 40	35	99.99%
Al_2O_3 200	3500 to 3900	Spherical	200	3.9	99.99%

5.3 Hardening

The hardening catalyzer used for the samples was Methyl Ethyl Ketone Peroxide (MEKP).

Table 2. Samples taken to Germany

Composition	Percentage	Sample Name
Pure UPR	-	B1
UPR + Al_2O_3 30-40	1%	A2
UPR + Al_2O_3 30-40	2.5%	A1
UPR + Al_2O_3 30-40	5%	A3
UPR + Al_2O_3 30-40	7.5%	A1
UPR + Al_2O_3 30-40	10%	C2
UPR + Al_2O_3 30-40	15%	E1
UPR + Al_2O_3 30-40	20%	A1
UPR + Al_2O_3 200	2.5%	A1
UPR + Al_2O_3 200	5%	A1
UPR + Al_2O_3 200	7.5%	A1
UPR + Al_2O_3 200	10%	A1
UPR + Al_2O_3 200	15%	A1

6. CHARACTERIZATION PROCESS

Thirteen samples were taken to the Institut fuer Hochspannungstechnik und Elektrische Energieanlagen (Elenia) of Technische Universitaet Braunschweig (TU-Braunschweig) from the Thermal Sciences Laboratory of Universidade Federal Fluminense for characterization. Table 2 lists the composition of the samples, percentage of fillers and sample name.

As the sample thickness of 12.7mm was too much for the experiments that would be done in Elenia, each one was sliced in two, making new samples with 4mm thickness.

Figure 2. New sliced samples

7. SCHERING BRIDGE

The Schering Bridge is an equipment used to determine the dissipation factor, also called tangent δ, and the electrical permittivity of a dielectric in a certain frequency. It is based on a bridge with three capacitors, two resistors and a null indicator. Figure 3 illustrates Schering Bridge's scheme.

An alternate high voltage electric potential, u(t) is applied to the bridge, more specifically to the capacitors C_x and C_2 in parallel. The parameters C_x and $\tan\delta_x$ represent the properties of the dielectric that are going to be determined, the capacitor C_2 and resistor R_4 are fixed and the values for R_3 and C_4 shall be adjusted with the support of the null indicator, N, in order to balance the bridge. When the null indicator reaches null value, the bridge is properly balanced. In other words, each side of the bridge has the same capacitance and resistance. Focusing on the parameter C_x, it is possible to demonstrate that:

$$C_x = \frac{\pi}{4}\epsilon_o\epsilon_r\frac{d^2}{h} \tag{6}$$

Where d is the diameter of the dielectric and h is its thickness. Also, the relation between C_x and C_2 can be defined
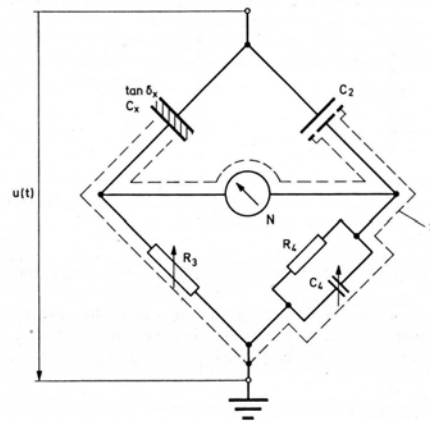
Figure 3. Schering Bridge's scheme (Kind and Feser, 2001)

as:

$$C_x = xC_2 \tag{7}$$

Therefore, equaling (6) and (7), an equation for the relative electrical permittivity can be deducted:

$$\epsilon_r = \frac{4hxC_2}{\pi\epsilon_o d^2} \tag{8}$$

7.1 Experiment settings

The Schering bridge used for this work belongs to Elenia Institute in the Laboratory for Insulators. It is shown on 4

Figure 4. Elenia's Schering bridge

In this equipment, the parameters for $\tan(\delta)$ and x should be adjusted with the support of the null indicator in order to balance the bridge.

In order to reduce the measurement error range and have more reliable results, each sample was tested with the Schering Bridge five times in different days.

The average time for testing each sample was around 30 seconds so, even though this experiment would be realized under high voltage conditions (around 3kV), the properties of the materials should not have changed.

The temperature of the Schering bridge chamber where the electrodes and samples would stay was 22 ± 2 °C and the relative humidity was 49 ± 3 %.

After measuring each sample, the results for tangent δ and x were stored in a spreadsheet and the electrical permittivity could be calculated through equation (8).

The final results were obtained after calculating the mean value between the five measured values for each sample and the mean value of the two samples of each material.

7.2 Results

Regardless of not measuring the pressure applied on the sample by the electrodes, it should be said that this pressure is known to influence the electrical characterization results. Hence, the higher the pressure, the higher the electrical properties values obtained from the characterization processes. No pressure was applied on the electrodes other than the one caused by the electrode weight

Bearing in mind the height of the samples ($h = 4$mm), the capacitance of the reference capacitor ($C_2 = 36.957$pF), the dielectric constant ($\epsilon_o = 8.854 \cdot 10^{-12}$As/Vm), the diameter between the outer side of the insulation ring on the electrode ($d = 37$mm) and the parameter x experimentally determined for each sample, the relative electrical permittivity of the samples could be calculated. It is important to emphasize that the experiments with the Schering Bridge were conducted at 50Hz frequency.

It should be comented that a relative electrical permittivity ratio was defined for the samples composed of UPR as matrix in order to ease the perception of the property enhancement with the increase in the filler concentration:

$$\epsilon_r^* = \frac{\epsilon_r}{\epsilon_{rUPR}} \tag{9}$$

7.2.1 UPR filled with aluminum oxide 30-40 nanoparticles

By looking into figure 5, it is possible to conclude that the $\tan(\delta)$ grows with the increase in fillers.
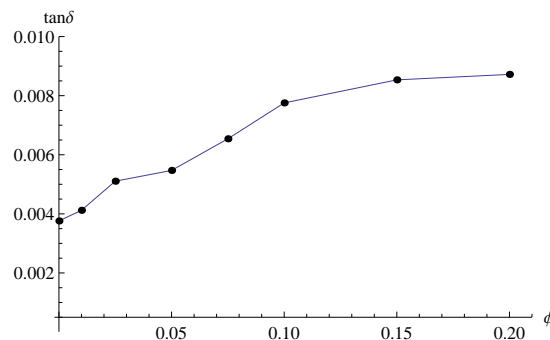

Figure 5. Dissipation factor versus filler concentration of UPR + Al$_2$O$_3$ 30-40 nanocomposites

Figures 6 and 7 were also plotted for a better comprehension of the relative permittivity variation.
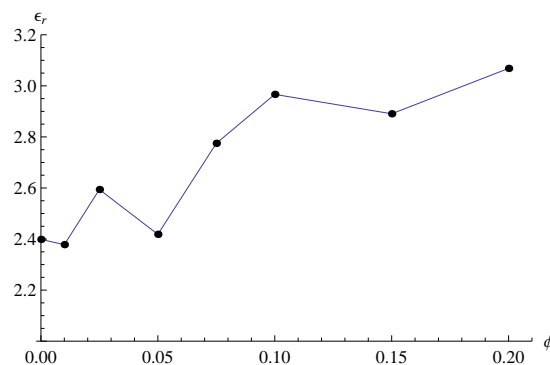

Figure 6. Relative electrical permittivity versus filler concentration of UPR + Al$_2$O$_3$ 30-40 nanocomposites

Analyzing the ϵ_r variation, it is possible to observe three peculiarities. The first one, would be the reduction on the relative electrical permittivity on the samples with 1% fillers if compared with the pure UPR samples. This can be explained because of the resistance in the charge transport through the polymer chains and interfaces of different materials (Singha and Thomas, 2008c). The new strong and stable boundaries of the filler and the matrix can reduce the
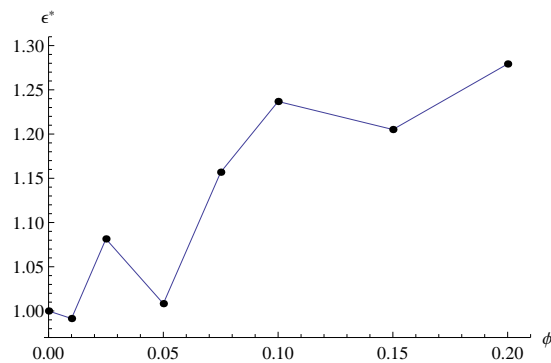
Figure 7. $\epsilon*$ versus filler concentration of UPR + Al_2O_3 30-40 composites

mobility of the polymer chains, reducing the free charge carriers and, consequently, reducing the electrical conductivity of the nanocomposite (Singha and Thomas, 2008a; Tsagarapoulos and Eisenberg, 1995; Mayes, 2005; Picu and Ozmusul, 2003). The other two peculiarities would be the reduction on the relative electrical permittivity of the samples with 5% fillers and 15% fillers. This could be explained due to a not so efficient mixture homogenization during the manufacturing process of the sample. Another explanation would be because of the presence of air bubbles trapped inside the sample. Since no vacuum was used during the manufacturing process of these samples and the relative electrical permittivity of the air is around 1.0006, air bubbles could have been trapped inside the sample, reducing the electrical permittivity of the sample.

7.2.2 UPR filled with aluminum oxide 200 nanoparticles

The Schering bridge results for the UPR filled with Al_2O_3 200 composites are presented on figures 8, 9 and 10.
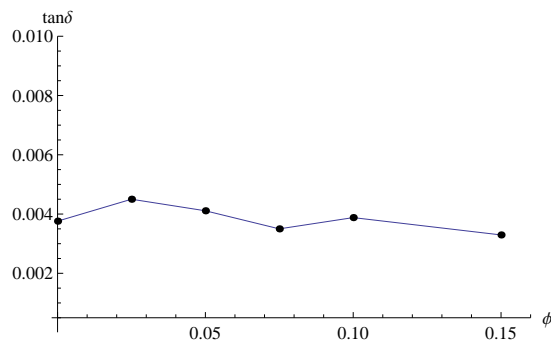

Figure 8. $\tan(\delta)$ versus filler concentration of UPR + Al_2O_3 200 composites

Even though the increase in the filler concentration should also increase the sources of charge carriers in the composite, these samples presented almost the same results for the dissipation factor. One reason for this peculiarity could be the fact that the Al_2O_3 200 nanoparticles may not as conductive as the Al_2O_3 30-40 ones. The other and most probable explanation would be that the ER samples are very porous and have many air bubbles trapped inside them.

With the exception of the samples filled with 5% nanoparticles, the results showed the expected raise in the relative electrical permittivity. These results may confirm a problem with the manufacturing process of the samples of ER and UPR filled with 5% of Al_2O_3 30-40 and 200.

8. GUARDED HEAT FLOW THERMAL CONDUCTIVITY METER

A guarded heat flow thermal conductivity meter is an equipment used to determine the thermal conductivity of a material by applying an one-dimensional heat flow. Basically, the material is put in an thermal insulating chamber and a temperature gradient is applied. The convection heat exchange between the side surface and the enviroment is modeled through Newton's Cooling Law as shown on figure 11. The temperature of this neighborhood is considered as the mean temperature of both surfaces and the insulation helps to keep this temperature and the temperature of the upper and bottom surfaces constant. Then, out of the heat balance equation, the thermal conductivity can be determined.
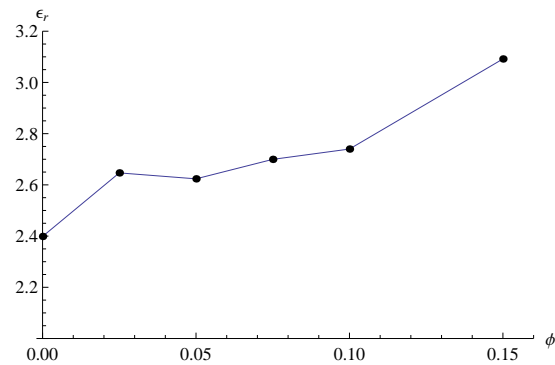
Figure 9. ϵ_r versus filler concentration of UPR + Al_2O_3 200 composites

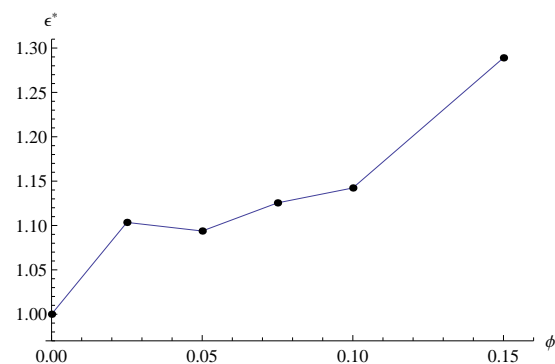Figure 10. $\epsilon*$ versus filler concentration of UPR + Al_2O_3 200 composites
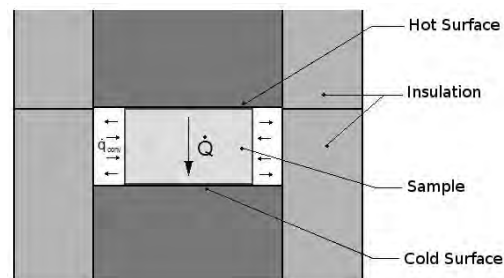

Figure 11. Guarded heat flow thermal conductivity meter chamber scheme (Moreira, 2011)

8.1 Experiment settings

The equipment used in these experiments was the Fox-50, manufactured by LasedComp. It is importat to emphasize that this equipment follows ASTM C518-04, E1530-06 and ISO 8301 standards. In order to make possible the variation of the hot and cold plates temperatures, a heat exchanger is conected to the Fox-50, in which a control system removes the extra heat. These temperatures are kept constant through peltier effect. Both equipments, the Fox-50 and the heat exchanger, are shown on figure 12.

A temperature variation of 20°C was set between the hot and cold plates and three mean temperatures were set to run the tests. Table 3 presents the target temperature values and also each plate temperature.

8.2 Contact thermal resistance

Due to the impossibility to determine the contact thermal resistance between the hot and cold plates and the sample, the contact thermal resistance was manually set to null and some Impastec IPT thermal paste was used in both sample surfaces. According to the manufacturer, the thermal conductivity of this thermal paste is 0.4W/mK.

Figure 12. LaserComp Fox-50 and the heat exchanger

Table 3. Temperature settings for tests

Target value (°C)	Lower plate (°C)	Upper plate (°C)
0	-10	10
25	15	35
50	40	60

8.3 Results

From equation (5), the following equation could be obtained to determine the thermal conductivity of the sample considering the thermal resistance of the thermal paste, the results obtained from Fox-50 and that the sample and the thermal paste are arranged in series:

$$k_s = L_s \left(\frac{k_t k_{tp}}{k_{tp} L_t - 2 k_t L_{tp}} \right) \tag{10}$$

Bearing in mind the lengh of the samples (L_s = 4mm), the aproximate lengh of the thermal paste (L_{tp} = 0.15mm), the total length of the system (L_t = 4.3mm), the thermal conductivity of the thermal paste (k_{tp} = 0.4W/mK) and the experimentally obtained thermal conductivity of the system (k_t), the thermal conductivity of each tested sample could be calculated.

A thermal conductivity ratio, k*, was used in these results in order to ease the perception of the property enhancement with the increase in the filler concentration:

$$k^* = \frac{k_s}{k_{UPR}} \tag{11}$$

It is important to emphasize that the pressurized air for the Fox-50 thermal insulating system would be kept around 60psi.

8.3.1 UPR filled with aluminum oxide 30-40 nanoparticles

As there is not much difference between the materials thermal conductivities at 0°C, 25°C and 50°C, only the results with the thermal conductivity ratio at 25°C was plotted.

From figure 13, it is possible to perceive a thermal conductivity gap with the 5% filled samples. This peculiarity was also present on the permittivity tests, confirming that either the mixture homogenization process was not so efficient or there are air bubbles trapped inside the sample or both cases. Besides, the expected evolution on the thermal conductivity with the increase in fillers can be seen.

8.3.2 UPR filled with aluminum oxide 200 nanoparticles

Like presented above, only the results with the k^* variation at 25°C are presented through figure 14.

It can be perceived that the maximum thermal conductivity raise for this filler was even bigger than the one reported for UPR samples filled with Al_2O_3 30-40, reaching an impressive 200%. This time, the results presented expected evolution on the thermal conductivity with the increase in fillers.
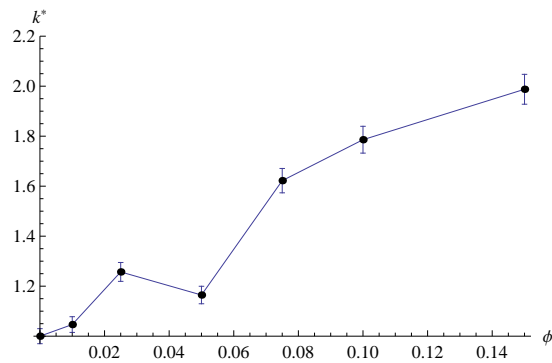
Figure 13. Thermal conductivity ratio variation at 25°C for UPR + Al_2O_3 30-40 nanocomposites
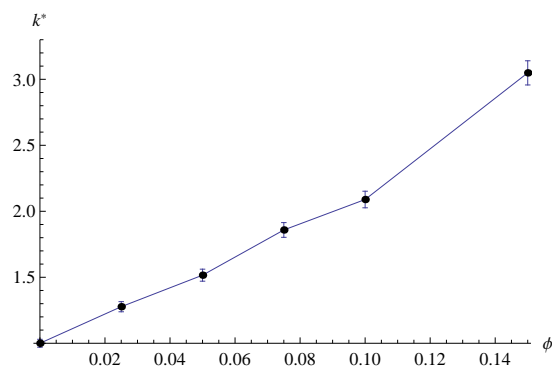

Figure 14. Thermal conductivity ratio variation at 25°C for UPR + Al_2O_3 200 nanocomposites

9. COMPARISON BETWEEN THERMAL AND ELECTRICAL PROPERTIES

In order to ease the perception of the property enhancement with the increase in the filler concentration, the results presented here compare the relative electrical permittivity ratio and the thermal conductivity ratio.

9.1 UPR filled with aluminum oxide 30-40 nanoparticles

In spite of the high concentrations of aluminum oxide nanoparticles, figure 15 shows that the electrical permittivity of the samples was raised by a maximum of only 25%. However, the thermal conductivity was raised by 100%. One of the reasons for this result is that the aluminum oxides are known for their low electrical permittivity and high thermal conductivity properties, so this confirmed what was expected. Also, a not so efficient mixture homogenization may produce abnormal results.
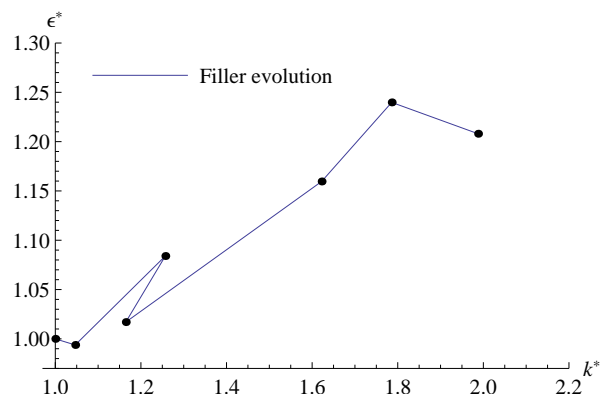

Figure 15. Variation of relative electrical permittivity with thermal conductivity ratios for UPR + Al_2O_3 30-40 nanocomposites

9.2 UPR filled with aluminum oxide 200 nanoparticles

Figure 16 presents the comparison between the relative electrical permittivity and the thermal conductivity ratios for UPR + Al_2O_3 200 nanocomposites
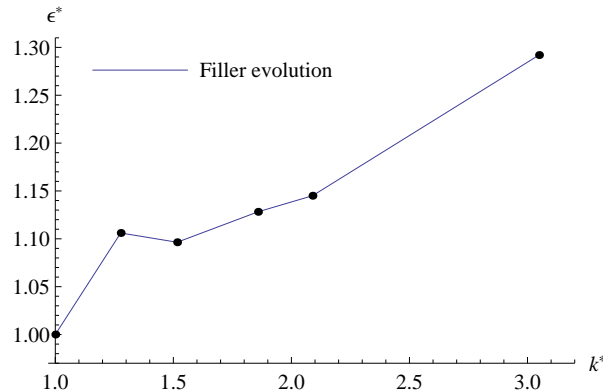

Figure 16. Variation of relative electrical permittivity with thermal conductivity ratios for UPR + Al_2O_3 200 nanocomposites

The results for the UPR filled with Al_2O_3 200 properties comparison followed the same pattern as those filled with Al_2O_3 30-40: a small raise in the electrical permittivity and a big raise in the thermal conductivity. However, it should be said that the expected constant raise in the properties with the addition of nanoparticles was not present, once the samples filled with 5% had lower electrical permittivity than those filled with 2.5%. As explained earlier, air bubbles trapped inside the sample have a big influence on the electrical permittivity, so this is probably the reason for this result.

10. CONCLUSIONS

Concerning the Schering bridge experiments, the samples could be tested and provided the electrical permittivity and dissipation factor under high voltage and at a frequency of 50Hz. Some samples presented unexpected results and the causes for these results were discussed. Three different explanations were proposed for different situations: the trapped air bubbles inside the sample, the not so efficient mixture homogenization and the strong and stable boundaries of the filler and the matrix.

Regarding to the thermal characterization, significant improvements in the nanocomposites thermal conductivity could be perceived. Even a small adition of 2.5% of nanoparticles was already enough to improve the thermal conductivity of the UPR filled with aluminum oxide nanoparticles by 30%. This can be explained due to the high thermal conductivity of these oxides.

The comparison between the thermal and electrical properties, more specifically between the thermal conductivity and the electrical permittivity, shows that despite the high concentrations of aluminum oxide nanoparticles raised the electrical permittivity by only 30% in UPR nanocomposites, the thermal conductivity presented an impressive raise of 200%. This can be explained due to the low electrical permittivity and high thermal conductivity of the metallic oxides or either the mixture homogenization process was not so efficient or there are air bubbles trapped inside the sample or both cases happened.

For future work, it would be interesting to compare the obtained results with the actual literature data, including other experimental work and data obtained from modeling in order to have a better global comprehension of the advantages and applicability of the tested nanocomposites. If possible, it would be good to analyze the nanocomposite samples with a Scanning Electron Microscope in order to confirm the theories of non-homogeneous dispersion of fillers. Last but not least, manufacturing new nanocomposite samples with different materials and extending the experiments to them would also help the research and development of the area.

Lastly, the results presented here are expected to be used as reference for the next works and should be able to help future research on nanocomposites applicability area, a new area of study in which there are not so many information and data to be based upon.

11. REFERENCES

Alston, L.L., 1968. *High-Voltage Technology*. Oxford University Press.
ASTM, 2006. "E2456 - Standard Terminology Relating to Nanotechnology".

Calabrese, C., Hui, L., Shchadler, L.S. and Nelson, J.K., 2011. "A review on the importance of nanocomposite processing to enhance electrical insulation". *IEEE Transactions on Dielectrics and Electrical Insulation*, Vol. 18, pp. 938–945.

Castellon, J., Nguyen, H.N., Agnel, S., Toureille, A., Fréchette, M., Savoie, S., Krivda, A. and Schmidt, L.E., 2011. "Electrical properties analysis of micro and nano composite epoxy resin materials". *IEEE Transactions on Dielectrics and Electrical Insulation*, Vol. 18, pp. 651–657.

Cha, H.G., Song, J., Kim, H.S., Shin, W., Yoon, K.B. and Kang, Y.S., 2011. "Facile preparation of fe2o3 thin film with photoelectrochemical properties". *The Royal Society of Chemistry*.

Chen, Y., Imai, T., Ohki, Y. and Tanaka, T., 2010. "Tree initiation phenomena in nanostructured epoxy composites". *IEEE Transactions on Dielectrics and Electrical Insulation*, Vol. 17, pp. 1509–1514.

Fan, L., Su, B., Qu, J. *et al.*, 2004. "Electrical and thermal conductivities of polymer composites containing nano-sized particles". In *Proceedings of the Electronic Components Conference*.

Hamming, L.M., Qiao, R., Messersmith, P.B. and Catherine Brinson, L., 2009. "Effects of dispersion and interfacial modification on the macroscale properties of tio2 polymer-matrix nanocomposites". *Composites science and technology*, Vol. 69, No. 11-12, pp. 1880–1886.

Kim, D., Lee, J.S., Barry, C.M.F. and Mead, J.L., 2007. "Microscopic measurement of the degree of mixing for nanoparticles in polymer nanocomposites by TEM images". *Microscopy research and technique*, Vol. 70, No. 6, pp. 539–546.

Kind, D. and Feser, K., 2001. *High Voltage Test Techniques*. Newnes.

Mayes, A.M., 2005. "Softer at the boundary". *Nature Materials*, Vol. 4, pp. 651–652.

Moreira, D.C., 2011. "Análise experimental de propriedades termomecânicas em nanocompósitos poliméricos".

Nelson, J.K., ed., 2010. *Dielectric Polymer Nanocomposites*. Springer.

Nguyen, M.Q., Malec, D., Mary, D., Werynski, P., Gornicka, B., Therese, L. and Guillot, P., 2010. "Silica nanofilled varnish designed for electrical insulation of low voltage inverter-fed motors". *IEEE Transactions on Dielectrics and Electrical Insulation*, Vol. 17, pp. 1349–1355.

Picu, R.C. and Ozmusul, M.S., 2003. "Structure of linear polymeric chains confined between impenetrable spherical walls". *J. Chem. Phys.*, Vol. 118, pp. 11239–11248.

Preetha, P. and Thomas, M.J., 2011. "Ac breakdown characteristics of epoxy nanocomposites". *IEEE Transactions on Dielectrics and Electrical Insulation*, Vol. 18, pp. 1526 – 1534.

Putjuso, T. and Sangarun, P., 2012. "Influence of annealing on the giant dielectric properties of cuo ceramics prepared by a simple pva sol-gel". *KKU Res. J.*, Vol. 17, No. 2, pp. 203–210.

Rong, M.Z., Zhang, M.Q. and Ruan, W.H., 2006. "Surface modification of nanoscale fillers for improving properties of polymer nanocomposites: a review". *Materials science and technology*, Vol. 22, No. 7, pp. 787–796.

Sarangi, P.P., Vadera, S.R., Patra, M.K., Prakash, C. and Ghosh, N.N., 2009. "Dc electrical resistivity and magnetic property of single-phase a-fe2o3 nanopowder synthesized by a simple chemical method". *Communications of the American Ceramic Society*, Vol. 92, No. 10, pp. 2425–2428.

Shinde, S.S., Bansode, R.A., Bhosale, C.H. and Rajpure, K.Y., 2011. "Physical properties of hematite a-fe2o3 thin films: application to photoelectrochemical solar cells". *Journal of Semiconductors*, Vol. 32, No. 1.

Singha, S. and Thomas, M.J., 2008a. "Dielectric properties of epoxy nanocomposites". *IEEE Transactions on Dielectrics and Electrical Insulation*, Vol. 15, pp. 12–23.

Singha, S. and Thomas, M.J., 2008b. "Permittivity and tan delta characteristics of epoxy nanocomposites in the frequency range of 1 mhzâĂŞ1 ghz". *IEEE Transactions on Dielectrics and Electrical Insulation*, Vol. 15, No. 1.

Singha, S. and Thomas, M.J., 2008c. "Reduction of permittivity in epoxy nanocomposites at low nano-filler loadings". In *Annual Report Conference on Electrical Insulation Dielectric Phenomena*. pp. 726–729.

Tjong, S.C., 2006. "Structural and mechanical properties of polymer nanocomposites". *Materials Science and Engineering: R: Reports*, Vol. 53, No. 3-4, pp. 73–197.

Tsagarapoulos, G. and Eisenberg, A., 1995. "Dynamic mechanical study of the factors affecting the two glass transition behavior of filled polymers. similarities and differences with random ionomers". *Macromolecules*, Vol. 28, pp. 6067–6077.

12. RESPONSIBILITY NOTICE

The following text, properly adapted to the number of authors, must be included in the last section of the paper:
The author(s) is (are) the only responsible for the printed material included in this paper.